Supplements

1 Background on the altimetry data from LEGOS

The altimetry data obtained from LEGOS come from the acquisitions of ENVISAT and Jason-2 radar altimetry missions on their nominal orbit (03/2002–10/2010 and 06/2008-10/2016 respectively). All the parameters necessary to estimate water levels (Crétaux et al., 2017) are contained in the Geophysical Data Records (GDR) made available by the space agencies. These data were obtained from Centre de Topographie des Océans et de l'Hydrosphère (CTOH - http://ctoh.legos.obs-mip.fr). Ranges used to derive altimeter heights are those processed using OCOG/Ice retracking algorithm (Wingham et al., 1986). Previous studies showed that altimeter heights derived using this retracking algorithm are more suitable for hydrological studies in terms of accuracy of water levels and availability of the data (Frappart et al., 2006;Santos da Silva et al., 2010;Sulistioadi et al., 2015) among the commonly available retracked data present in the GDRs.

The Multi-mission Altimetry Processing Software (MAPS) was used to visualize and process the altimetry data in order to obtain the virtual stations (VS) at the cross-sections between the altimeter ground tracks and the rivers (Frappart et al., 2015;Normandin et al., 2018). Data processing is composed of three main steps: (i) a coarse delineation of the VS using Google Earth; (ii) a refined selection of the valid altimetry data based on visual inspection; and (iii) the computation of the time series of water level. The altimetry-based water level is computed for each cycle using the median of the selected altimetry heights, along with their respective deviation (i.e., mean absolute deviation). This process is repeated each cycle to construct the water level time series at the virtual stations; see Frappart et al., 2015; Normandin et al., 2018 for more details.

Literature

Crétaux, J.-F., Nielsen, K., Frappart, F., Papa, F., Calmant, S., and Benveniste, J.: Hydrological applications of satellite altimetry: rivers, lakes, man-made reservoirs, inundated areas, in: Satellite Altimetry Over Oceans and Land Surfaces; Earth Observation of Global Changes, edited by: Stammer, D., and Cazenave, A., CRC Press, Boca Raton, FL, USA, 459–504, 2017.

Frappart, F., Calmant, S., Cauhopé, M., Seyler, F., and Cazenave, A.: Preliminary results of ENVISAT RA-2-derived water levels validation over the Amazon basin, Remote Sensing of Environment, 100, 252-264, https://doi.org/10.1016/j.rse.2005.10.027, 2006.

Frappart, F., Papa, F., Marieu, V., Malbeteau, Y., Jordy, F., Calmant, S., Durand, F., and Bala, S.: Preliminary Assessment of SARAL/AltiKa Observations over the Ganges-Brahmaputra and Irrawaddy Rivers, Marine Geodesy, 38, 568-580, 10.1080/01490419.2014.990591, 2015.

Normandin, C., Frappart, F., Telly Diepkilé, A., Marieu, V., Mougin, E., Blarel, F., Lubac, B., Braquet, N., and Ba, A.: Evolution of the Performances of Radar Altimetry Missions from ERS-2 to Sentinel-3A over the Inner Niger Delta, 833 pp., 2018.

Santos da Silva, J., Calmant, S., Seyler, F., Rotunno Filho, O. C., Cochonneau, G., and Mansur, W. J.: Water levels in the Amazon basin derived from the ERS 2 and ENVISAT radar altimetry missions, Remote Sensing of Environment, 114, 2160-2181, https://doi.org/10.1016/j.rse.2010.04.020, 2010.

Sulistioadi, Y. B., Tseng, K. H., Shum, C. K., Hidayat, H., Sumaryono, M., Suhardiman, A., Setiawan, F., and Sunarso, S.: Satellite radar altimetry for monitoring small rivers and lakes in Indonesia, Hydrol. Earth Syst. Sci., 19, 341-359, 10.5194/hess-19-341-2015, 2015.

Wingham, D., Rapley, C., and H D, G.: New Techniques in Satellite Altimeter Tracking Systems, 1986.

2 Model parameter ranges and constrains

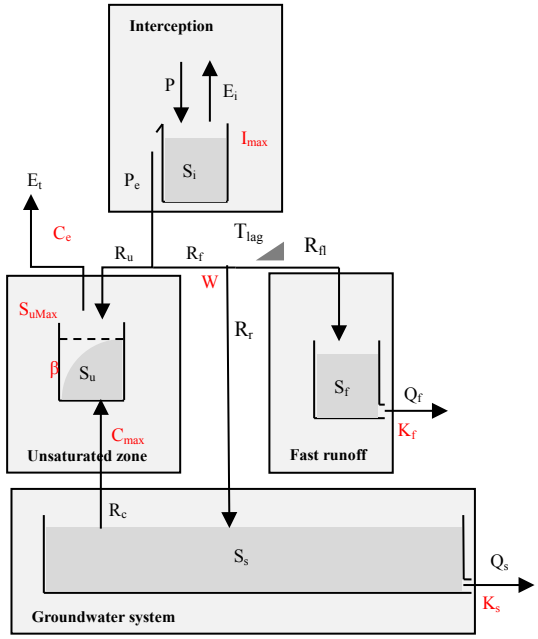

Figure S1: Model structure. Parameters are marked in red, storages and fluxed in black. Symbol explanation: Fluxes [mm d^{-1}]: precipitation (P), effective precipitation (P_e), potential evaporation (E_p), interception evaporation (E_i), plant transpiration (E_t), infiltration into the unsaturated zone (R_u), drainage to fast runoff component (R_f), delayed fast runoff (R_{fl}), groundwater recharge (R_r), upwelling groundwater (R_c), fast runoff (Q_f), groundwater/slow runoff (Q_s), total runoff (Q_m). Storages [mm]: storage in interception reservoir (S_i), storage in unsaturated root zone (S_u), storage in groundwater/slow reservoir (S_s), storage in fast reservoir (S_f). Parameters: interception capacity (I_{max}) [mm], maximum upwelling groundwater (C_{max}) [mm d^{-1}], maximum root zone storage capacity (S_{umax}) [mm], splitter (W) [-], shape parameter (β) [-], transpiration coefficient (C_e) [-], time lag (T_{lag}) [d], reservoir time scales [d] of fast (K_f) and slow (K_s) reservoirs.

Table S1: Model parameter values and ranges. See Figure S1 for the parameter explanation and Table S2 for the parameter constrains applied during the random parameter generation.

Landscape class	Parameter	min	max	Unit
Entire catchment	K_s	100	100	d
	C_e	0.5	0.5	-
Flat	I_{max}	0	2	mm d^{-1}
	S_{umax}	200	2000	mm
	β	0	0	-
	T_{lag}	0	0	d
	K_f	10	12	d
	W	0.1	0.5	-
	C_{max}	0	0	mm d^{-1}
Sloped	I_{max}	0	2	mm d^{-1}
	S_{umax}	200	2000	mm
	β	0	2	-
	T_{lag}	1	5	d
	K_f	10	12	d
	W	0.1	0.5	-
	C_{max}	0	0	mm d^{-1}
Wetland	I_{max}	0	2	mm d^{-1}
	S_{umax}	200	2000	mm
	β	0	0	-
	T_{lag}	0	0	d
	K_f	10	12	d
	W	0.1	0.5	-
	C_{max}	0.1	2	mm d^{-1}
River profile	v	0.01	5.0	m s^{-1}
	k	5	45	$m^{1/3}$ s^{-1}
	a	0.1	800	m^3 s^{-1}
	b	1	3	-

Table S2: Parameter constrains. See Figure S1 for the parameter explanation.

Parameter	Constrain
Maximum root zone storage capacity	$S_{umax\ sloped} > S_{umax\ flat}$
	$S_{umax\ sloped} > S_{umax\ wetland}$
Maximum interception	$I_{max\ sloped} > I_{max\ flat}$
	$I_{max\ sloped} > I_{max\ wetland}$
Splitter for groundwater percolation	$W_{sloped} > W_{flat}$

3 Characteristics of the virtual stations

Table S3: Characteristics of the virtual stations in the Luangwa River basin for which remotely sensed river water levels are available: station ID, coordinates (X, Y), river slope (*i*), river width (*B*), river bank slopes (i_1 and i_2), upstream catchment area, acquisition date of the image in Google Earth used to extract the river geometry information, and discharge at Luangwa Bridge gauge station (basin outlet; absolute values and relative to the maximum discharge); in the absence of discharge data on the acquisition dates, the long-term mean daily values for the entire time period available were used.

VS	X	Y	i [-]	B [m]	i_1 [-]	i_2 [-]	A [m^2]	Acquisition date	$Q_{absolute}$ [$m^3 s^{-1}$] ($Q_{relative}$ [%])
1	30.2823°	-14.8664°	0.00049	324	36	29	10211995771	13-9-2010	68 (1%)
2	30.0864°	-14.366°	0.00062	7	17	83	14859805930	13-10-2013	65 (1%)
3	32.1715°	-12.4123°	0.00019	3	19	42	44337218380	17-12-2013	211 (4%)
4	31.1868°	-13.5927°	0.00020	129	42	8	87227195673	5-6-2013	160 (3%)
5	31.6984°	-13.2039°	0.00020	185	31	20	78090945429	20-9-2013	60 (1%)
6	32.2998°	-12.2007°	0.00039	170	30	17	40935244516	13-6-2013	146 (3%)
7	32.2805°	-12.1157°	0.00030	78	38	77	40747298483	13-6-2013	146 (3%)
8	32.831°	-11.3674°	0.00031	10	48	21	21066101487	26-9-2013	97 (2%)
9	30.2704°	-14.8809°	0.00017	99	8	5	102140213550	14-11-2009	30 (1%)
10	31.78405°	-13.0995°	0.00029	100	26	20	77559639645	26-7-2013	89 (2%)
11	31.71099°	-13.1943°	0.00020	54	34	30	78051272962	20-9-2013	60 (1%)
12	30.2740°	-14.8763°	0.00017	82	8	15	102135928406	14-11-2009	30 (1%)
13	32.15843°	-12.412°	0.00019	87	43	30	44340963341	17-12-2013	211 (4%)
14	32.15989°	-12.4127°	0.00019	128	83	19	44339840479	13-6-2013	146 (3%)
15	30.2740°	-14.8763°	0.00017	82	8	15	102139379771	13-6-2013	146 (3%)
16	32.16056°	-12.4125°	0.00019	128	83	19	44339840479	17-12-2013	211 (4%)
17	31.80001°	-13.0909°	0.00029	86	21	83	77553414963	13-6-2013	146 (3%)
18	30.61577°	-14.1852°	0.00051	227	24	20	96231647197	20-9-2014	60 (1%)
Outlet	30.21491°	-14.96678°	0.00037	149	8.62	10.10	154325857000	26-7-2016	89 (2%)

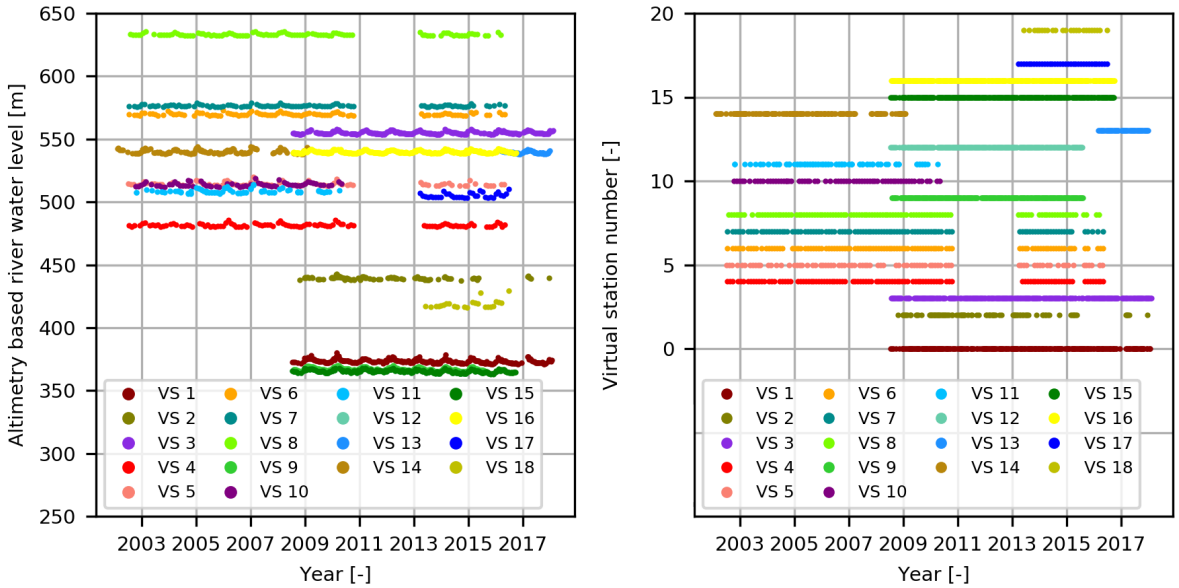

Figure S2: Visualisation of the altimetry time series relative to a reference ellipsoid (left) and altimetry data availability (right) for all virtual stations used in this study. The colours for the individual stations correspond with those in Figure 1 and 3.

4 Influence of the number of good virtual stations used for calibration/validation

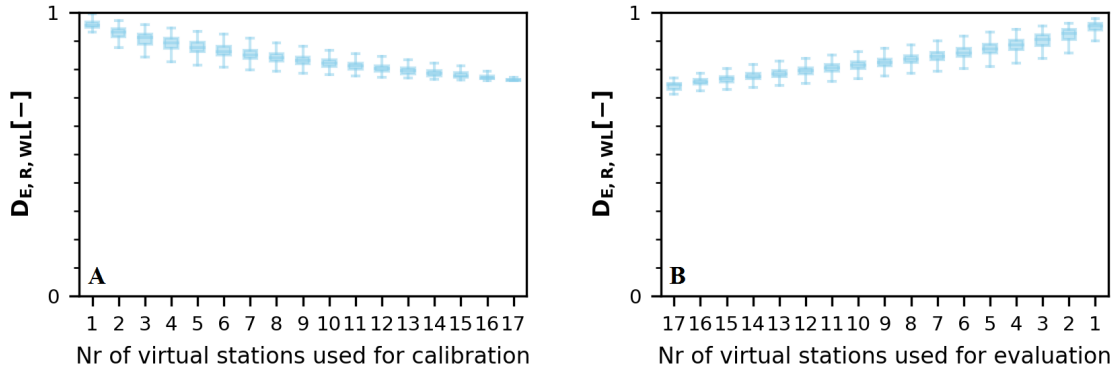

Figure S3: Influence of the number of virtual stations used for A) model calibration and B) evaluation on the model performance $D_{E,R,WL}$ applying Altimetry Strategy 1.

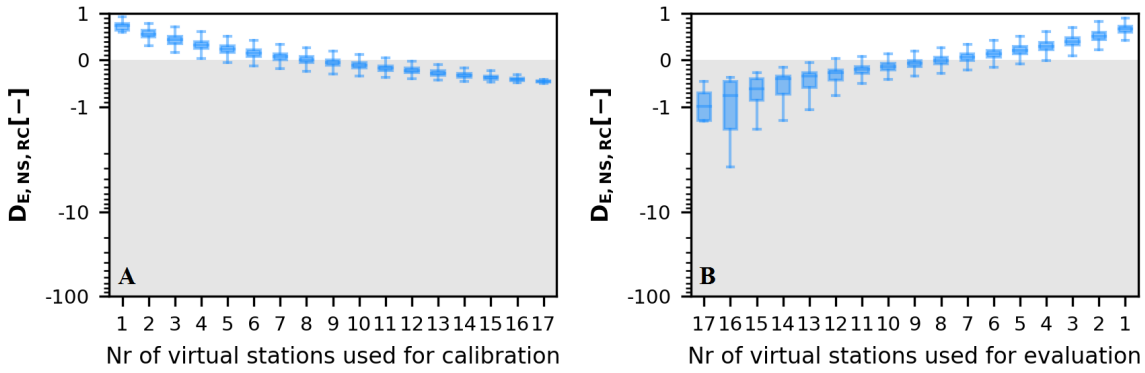

Figure S4: Influence of the number of virtual stations used for A) model calibration and B) evaluation on the model performance $D_{E,NS,RC}$ applying Altimetry Strategy 2.